Chemical Physics 463 (2015) 111–119

Contents lists available at ScienceDirect

Chemical Physics

journal homepage: www.elsevier.com/locate/chemphys

Branching and competition of ultrafast photochemical reactions of cyclooctatriene and bicyclooctadiene

Kyriaki Kosma [1], Sergei A. Trushin, Wolfram E. Schmid [2], Werner Fuß *

Max-Planck-Institut für Quantenoptik, 85741 Garching, Germany

ARTICLE INFO

Article history:
Received 25 August 2015
In final form 13 October 2015
Available online 23 October 2015

Keywords:
Pericyclic reactions
Hula twist
Potentials
Bright and dark states
Concertedness

ABSTRACT

The main primary photoproducts of cycloocta-1,3,5-triene (COT) are a strained *mono-E* isomer, *Z,Z*-octatetraene (OT, from electrocyclic ring opening) and benzene + ethylene. We investigated the excited-state dynamics of COT by time-resolved mass spectroscopy, probing by near-IR photoionization. Unexpectedly, we found only one reaction channel. We assign it to the pericyclic reactions. Evidence for an early branching between this and the Z–E channel is taken from previous resonance Raman data. This channel confirms previously formulated rules on the excited states involved, the reaction path and driving forces and contributes to their rationalization. Bicyclo[4.2.0]octa-2,4-diene undergoes only two pericyclic reactions: ring opening to OT and cleavage to benzene + ethylene. We investigated it briefly in its equilibrium mixture with COT. The data are consistent with a common path on the excited surfaces. Suggestions are made for structures of conical intersections, and driving forces are considered. All processes were found to be barrierless.

1. Introduction

The modern description of photochemical pericyclic reactions [1,2] is based on the following concepts: After vertical excitation of a polyene to the so-called spectroscopic state ($1B_2$ in the frequent molecular symmetry C_{2v}) the molecule is first accelerated along Franck–Condon (FC) active coordinates, which mainly involve the lengths and torsion angles of conjugated π bonds. Thereafter the Woodward–Hoffmann (WH) type σ–π interactions can begin, so that the motion continues on the same electronic surface in a (slightly) different direction towards a conical intersection (CI) with a two-electron excited ("dark", $2A_1$ in C_{2v}) state. This state involves the same two orbitals as $1B_2$ (but with both electrons lifted up), which are just those that cross each other in the WH-type orbital correlation diagram. The orbital crossing causes an avoided crossing of the $2A_1$ and $1A_1$ potentials. The resulting $2A_1$ minimum ("pericyclic minimum" [1,2], which may actually be a saddle point) is lower in energy and more shifted in WH direction than the $1B_2$ minimum. Even further down is a conical intersection (CI) with the ground state ($2A_1/1A_1$ CI). It is typically displaced into a symmetry-breaking direction. The wave packet hence moves from the $1B_2$ surface around the first CI via the $2A_1$ minimum (acting as a collection well) or directly to the funnel ($2A_1/1A_1$ CI), where it branches to the product(s) and the reactant in their ground states.

This view resulted in particular from quantum chemical (e.g. [2,3]) and time-resolved (e.g. [2,4]) investigations of the electrocyclic ring opening of 1,3-cyclohexadiene. (For more literature, see the two reviews [5,6].) A similar scheme with spectroscopic state, dark state and conical intersections is valid for cis–trans isomerizations of polyenes [7,8]. The majority of the pericyclic and cis–trans isomerizations investigated turned out to be barrierless and hence ultrafast (see the recent compilation in [9]).

Ring opening is practically the only photochemical process of cyclohexadiene, not counting the return from the last CI to the reactant (i.e., internal conversion). On the other hand, there are many molecules exhibiting more than one photochemical reaction at a given excitation wavelength. It seems interesting, where on the potentials the branching(s) occur. One possibility is the FC region; previously this was implicitly assumed in many photochemical investigations, where only states were considered instead of potentials and the paths on them. On considering also the slopes of potentials in this region, it was just recently shown that one can in fact understand a wide variety of the observed selections between different allowed (sometimes also forbidden) pericyclic reactions and cis–trans isomerizations and other phenomena such

* Corresponding author at: Weidachstr. 12, 85748 Garching, Germany.
E-mail addresses: kosma@iesl.forth.gr (K. Kosma), sergei.a.trushin@mpq.mpg.de (S.A. Trushin), w.fuss@mpq.mpg.de (W. Fuß).
[1] New address: Institute of Electronic Structure and Laser (IESL), Foundation for Research and Technology-Hellas (FORTH), 71110 Heraklion, Crete, Greece.
[2] New address: Gertrud-von-le-Fort-Str. 38, 97074 Würzburg, Germany.

http://dx.doi.org/10.1016/j.chemphys.2015.10.007
0301-0104/

as wavelength dependences [9]. However, also other features later on the surfaces such as ridges and conical intersections are natural branching regions, and the local geometrical structures are usually correlated with the course of the reactions. For example, the cis–trans isomerization and H migration in ethylene and derivatives were suggested to originate from a common CI (or intersection region), in which the two reactions are both half finished [10] (see there for more examples and previous suggestions). We suggest both an early and a late branching for a compound (cyclooctatriene) investigated here.

In this work we use femtosecond-time-resolved mass spectroscopy in the gas phase to study cycloocta-1,3,5-triene (COT) and briefly also its thermal isomer bicyclo[4.2.0]octa-2,4-diene (BCOD). Both molecules show several pericyclic reactions, and COT has a strained *mono-E* isomer even as the main product (Scheme 1, where isomerization at the central double bond was assumed, see Section 4.4). Only flash spectroscopy [11] and matrix isolation [12,13] identified the primary products shown in Scheme 1. Because at room temperature the strained product *mono-E*-COT in the ground state forms *Z,Z*-OT in milliseconds and *Z,Z*-OT closes the ring again within seconds to COT [11], preceding works observed only minor side products and secondary photoproducts (such as trans isomers of OT and others, not shown in the Scheme; see, for example, [14] for an early careful investigation and p. 248 of [15] for a summary including primary products). The photochemical primary products of BCOD are benzene + ethylene and octatetraene [12]. On prolonged storage COT equilibrates in a thermally allowed electrocyclic reaction with BCOD [16,17] (after longer time or at higher temperatures also with cycloocta-1,3,6-triene via sigmatropic 1,5-migration of H [14,17]. All these isomers can also be formed already in the preparation by reduction of cyclooctatetraene [18].). COT can be isolated via its $AgNO_3$ complex, from where it can again be displaced by concentrated ammonia [16]. We mainly investigated COT prepared in this way, but did some measurements also with the commercial COT/BCOD mixture, so that some conclusions on BCOD are also possible.

The experimental technique is described in our cyclohexadiene work [19], for instance. Briefly, the third harmonic (270 nm) of a Ti-sapphire laser excites the molecules in the gas phase and the fundamental (810 nm) probes them with varying time delay by nonresonant photoionization; the parent and fragment ions are detected depending on this delay. The ionic fragmentation strongly increases, the more energy is released on the path of the wave packet (in the form of kinetic energy) and the more it is displaced; this is because the ionization is vertical, thus conserving the kinetic energy and geometric structure. This rule is not only an assignment help but also provides the chance to extract many time constants, if many fragment ions are recorded. This possibility is important, if one wants to record several processes (photochemical reactions), each of which consisting of more than one step.

Previously we were frequently able to record several branched processes, for example in cyclohepta- and cycloocta-1,3-diene [20], which both undergo Z–E-isomerization and an electrocyclic reaction (ring closure to cyclobutene derivatives). However, in the present work we found less time constants for COT than expected. Perhaps some parallel processes have characteristic times too similar to be distinguished, or alternatively the ionization probability from one of the paths is too small (see Section 4).

A previous attempt at time-resolved mass spectroscopy of COT was unfortunately done with the unseparated mixture [21]. The kinetic analysis was also oversimplified, so that only a limited comparison with the present work is possible. Except COT → OT, the correct reactions were also not recognized. However, valuable complementary information is available from the resonance Raman work of the Mathies group [22–26]; in particular the intensity analysis [22] provided the direction of initial motion, even if

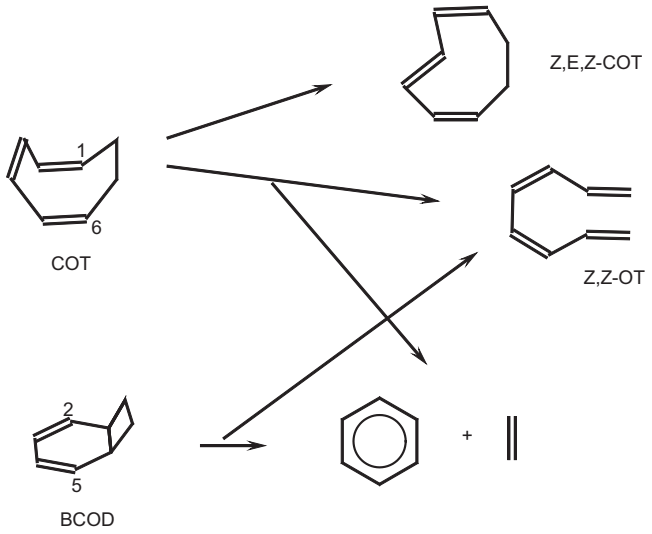

Scheme 1. Primary photoreactions of cyclooctatriene (COT) and bicyclooctadiene (BCOD) according to [11,12]. It is here assumed (see Section 4.4) that it is the central double bond, which rotates to produce the strained isomer. The arrows also hint to the suggested early and late branchings.

the authors only considered COT → OT as reaction. As revealed by the present work, the time resolution (several ps) in this Raman work [26] was, however, not sufficient for the dynamics of these processes. A time-resolved electron diffraction study with its resolution of only 4 ps also did not show the evolution on the potentials but only one of the (primary) products, *Z,Z*-OT and its ground-state rotamerization [27].

For labeling the spectroscopic, the dark and the ground state, we use the symmetry types of C_{2v} ($1B_2$, $2A_1$ and $1A_1$) as in [22–26], who point to the approximate local symmetry of the π system. Actually COT is a twisted boat (with two enantiomeric potential minima) [28,29] and has hence no symmetry (C_1), whereas BCOD has one symmetry plane (C_s).

2. Experimental

The COT/BCOD mixture was purchased from Organometallics (East Hampstead, USA). According to gas-chromatographic mass-spectroscopic analysis, it contained about 20% BCOD besides the COT. The monocyclic compound was isolated from the mixture according to the procedure of [16]: by complexing it with $AgNO_3$ (1.6 mol per mol of isomers) dissolved in water (30% solution). The precipitate was twice recrystallized from ethanol. From a small sample, COT was displaced by concentrated aqueous ammonia, as in [16]; thereafter, no organic impurity was detectable gas-chromatographically. The main part of the COT was, however, recovered in a simpler way: by decomposing the complex in vacuum at 60–80 °C (1 h), collecting the volatiles in a cold trap. The condensate also showed no BCOD (<0.1%), though it contained traces of water and ethanol. As the latter do not absorb the pump radiation in the near UV and the ions would be easy to distinguish from COT^+, the sample was used in the experiment without drying.

COT and the unseparated COT/BCOD mixture were investigated at 20 °C in the gas phase. They were introduced through a precision needle valve to the ionization region of a time-of-flight mass spectrometer at a pressure of $\approx 10^{-7}$–10^{-6} mbar, where they were first excited by a weak pump pulse at 270 nm (duration ≈28 fs, intensity $\approx 10^9$ W cm^{-2}) and then ionized with the delayed probe laser at 810 nm (≈17 fs, $\approx 10^{13}$ W cm^{-2}). (The pump wavelength is within the first strong UV band of both compounds [16].) The probe radiation was generated by shortening of pulses from a

Ti-sapphire laser system (Spectra Physics Tsunami + Spitfire, 2 mJ, 45 fs, 1 kHz) via self-focusing in argon and compressing the resulting pulses by reflection at chirped mirrors [30]. The pump radiation was produced by frequency tripling in a short argon cell; details are described in [30], where the method was further optimized. To compensate the lengthening caused by propagation in air, these pulses were shortened by a prism compressor to 28 fs [30]. (In later experiments, a vacuum beam path was used after tripling, so that the pulse lengths could be used and maintained around 11 fs, see e.g. [4,35].) Varying the pump–probe delay time, ion yields were measured mass-selectively by a time-of-flight mass spectrometer. Pump and probe polarizations were in general used with an angle of 55° ("magic angle") to avoid effects induced by molecular rotation, except for some investigations at shorter times (<100 fs), where interference by the much slower rotations (predicted time constants $\tau_r = 602$, 634 and 847 fs, calculated from the inertial moments as in [31]) is not expected. In each pulse two ion signals were simultaneously measured by two boxcar integrators: besides an ion from COT or BCOD also $Cr(CO)_6^+$ which is generated by (1 + 3)-multiphoton ionization of added $Cr(CO)_6$. Subtracting a small delay (12 fs, corresponding to the lifetime of $Cr(CO)_6$ in the initially excited state [32]) versus the time zero, found from the Xe^+ signal in separate experiments, the $Cr(CO)_6^+$ data directly yield the instrumental function, i.e., the correlation function of the pump with the third power of the probe. (The ionization energy of COT of 8.4 eV [33] requires nominally 5.5 fundamental photons or one of the third harmonic and 2.5 of the fundamental.) In the Supporting Information we show the Xe^+ and $Cr(CO)_6^+$ signals. The instrumental function derived from the latter is a Gaussian with halfwidth 30 fs. It was used to calculate the length of the pump pulse and for deconvoluting short-time signals. It also served for synchronization of different scans. Details of the setup are given in [19].

3. Results

The conventional (electron-impact) mass spectra of COT and BCOD show the parent ion (M^+, $C_8H_{10}^+$, mass 106 u) and $M^+ - 1$ with relative intensity about 20% besides the fragments $C_7H_7^+$ (91 u, 50%) and $C_6H_6^+$ (78 u, 100%) and several smaller fragments. In the ionization by 1 pump + ≥3 probe photons, the mass spectrum depends not only on the delay time and the internal state of the molecule (which is the basis of the time-resolved mass spectroscopy) but also on the probe intensity: by lowering the latter, fragmentation can be strongly reduced [21]. In view of the valuable information contained in the fragment signals, we preferred higher probe intensities (near 10^{13} W cm^{-2}), where fragmentation was similarly strong as in the conventional spectrum.

Mainly the parent ion and the strongest fragment (78 u) were studied with time resolution. Because the signals with masses 91 and 105 (shown in the Supporting Information) are very similar to that of mass 78 and do not provide additional time constants, we did not investigate them further. The time constants were the same, when the probe intensity was varied by a factor of 2.7, although the signal shapes (relative intensities of tails versus maxima) changed considerably, as expected, because the order of ionization rises, when the molecule relaxes down the potential surfaces.

In the analysis of the time-resolved data, the simplest assumption is that population flows over several locations L_i on the potential surfaces and that this flow can be described by rate equations. Their solution for the L_i populations results in sums of exponentials with time constants τ_i, no matter whether the processes are purely consecutive or partially branched; only the interpretation of the pre-exponential coefficients (with relative L_i populations multiplied by ${}^m\sigma_i$) differs for the two cases. The ${}^m\sigma_i$ represent the mass spectrum associated with the location L_i. In addition to an irreversible population flow, vibrations in L_i can occur and can periodically modulate the ${}^m\sigma_i$ (probability to produce an ion of mass m from location i). Hence the signals are simulated by a sum of exponentials (fit parameters: pre-exponential factors containing ${}^m\sigma_i$ and the time constants τ_i in the exponents) multiplied by functions

$$f_{osc} = 1 + A\exp(-t/t_d)\cos(2\pi\nu t - \varphi) \quad (1)$$

which contain the oscillation frequency ν, its phase φ, the pure dephasing time t_d and the modulation depth A as fit parameters. (Such vibrations imply the directions of local slopes on the potentials, see Section 4.1.) To simulate the signal also during the pump–probe overlapping time (<30 fs), these sums of (modulated) exponentials must be convoluted with the (Gaussian) pump and probe pulses, i.e. the instrumental function. In practice, one first fits a sum of exponentials (with convolution, if necessary) to the measured signals, then divides the latter by the former and takes the Fourier transform of the result (diminished by 1) to get the frequencies. These are entered into functions of type (1), which are then multiplied by the (convoluted) sum of exponentials; this complete function is then fitted to the measured data to get also the parameters A and φ and a final correction of the time constants τ_i and cross sections ${}^m\sigma_i$. Each τ_i and oscillation frequency ν_i in general appear in more than one signal, so that they can be cross-checked. Details of the evaluation are given in [19,34,35], in particular in the presence of oscillations in [34,35].

3.1. Cyclooctatriene

Fig. 1 shows examples of time-resolved data of the parent ion (mass 106 u, panel a) and the fragment with mass 78 (panel b) together with fit curves. The fitted time constants and oscillation parameters are listed in Table 1. The parent decays to zero (that is to the level at negative delay times), whereas there is a small positive pedestal at long times in the fragment signals (subtracted in Fig. 1(b)). It is obvious that the parent signal decays with at least two time constants. Comparison with the fragment, however, reveals that a satisfactory simulation requires two such times (10 and 11 fs) already in the early region (see the Supporting Information, where the time resolution is also discussed). This would be hard to interpret (see Section 4). Therefore we prefer to simulate this part by an exponential decay ($\tau_1 = 11$ fs) superimposed by a low-amplitude oscillation (period $T_{osc1} = 34$ fs) with very short dephasing time (18 fs). (Such a rapid dephasing can arise from a fast change of the vibrational frequency along the path, as previously found in butadiene [36] or metal carbonyls [35], for example.) Especially where obscured by convolution with the pump and probe pulses (times <30 fs), such a strongly damped oscillation cannot be distinguished from an exponential decay. The slower part can be reproduced by a purely exponential decay ($\tau_2 = 67$ fs). However, because a weak oscillation ($T_{osc2} = 200$ fs) appeared in the corresponding observation window (L_2) of the fragment 78, we allowed such an oscillation (period fixed to 200 fs) also for the parent. In fact, the fit improved noticeably thereby, without change of τ_2. More importantly, an inconsistency was practically removed between data such as Fig. 1(a) and those measured over a shorter time range (≤200 fs): If L_2 was measured over a time $\ll T_{osc}$, the fit program added the clipped oscillation to the nonperiodic (exponential) part, with the result of a too short τ_2.

We did not try to reduce the error limits by more averaging, because the conclusions do not depend on the exact numerical values. The estimated error limits of Table 1 are based on several data sets, not only those of Fig. 1. A weak higher-frequency oscillation in L_3, visible near 300 fs in Fig. 1(b), seems to be spurious: It does not show up in the Fourier transform (see Supporting Information,

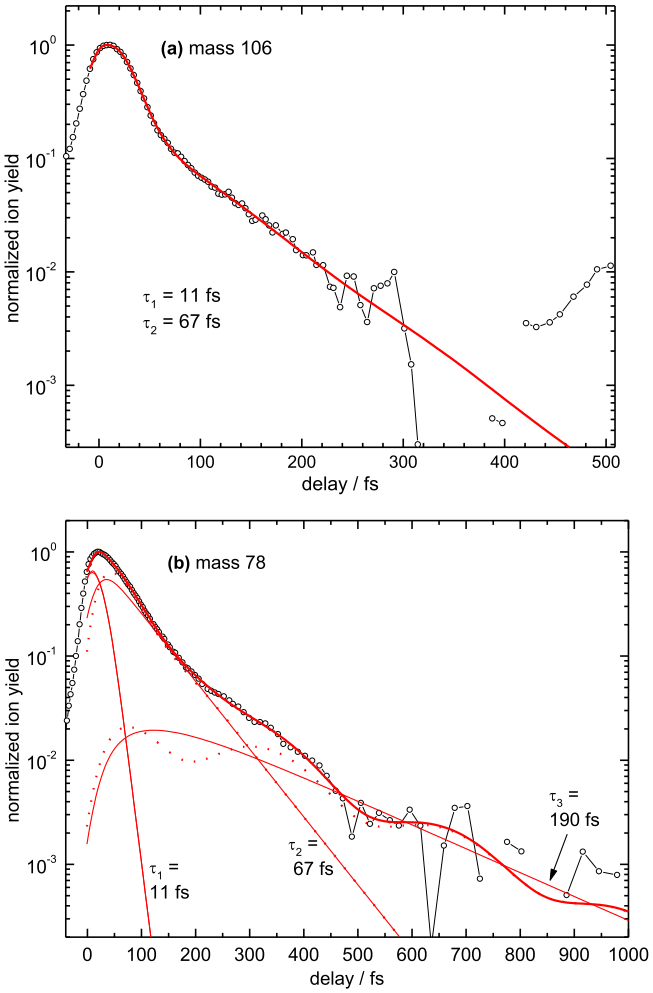

Fig. 1. Time dependent signals (symbols) and their simulations (smooth lines) for the parent (a) and a fragment ion (b) of COT. In addition to data and full simulation, panel (b) also shows the additive signal contributions from L_1, L_2 and L_3 (thin lines). For the latter two, the exponential parts (from the decaying L_2 and L_3 populations, thin lines) are displayed separately from those including the periodic modulation of the ionization probability (dotted lines). For L_1, the oscillatory part is too small to show.

where also the oscillations are separated from the exponential part).

The fragment shows – after an initial decay with the same τ_1 and τ_2 as the parent – also a third time constant (τ_3 = 190 fs). In this observation window, the signal is strongly modulated by an oscillation (T_{osc3} = 330 fs). Also in the preceding window the simulation improved on adding a weak oscillation (period ca. 200 fs). For the first window, we used the same τ_1 and oscillation as for the parent. Fig. 1(b) also shows the more important components of the simulation: the three exponential parts and for the second and third window also the decays modulated by the oscillations. Table 1 summarizes the fit results.

The pedestal of the mass-78 signal was subtracted from the data shown in Fig. 1(b) (to better visualize the exponential parts), although fitting was done without subtraction. Up to 6 ps it remains constant and does not show any signs of decay.

As already said, the fragments with mass 91 and 105 were only briefly investigated. They could be fitted with parameters identical to those of mass 78 and are therefore not reported here; some data are, however, reported in the Supporting Information.

3.2. Cyclooctatriene/bicyclooctadiene mixture

According to the UV spectrum in [16], COT and BCOD have practically the same absorption cross section at the pump wavelength (270 nm). As BCOD is present with about 20% in the mixture, its contribution to the signals may therefore be noticeable.

As explained in the Discussion, the excited-state path for BCOD is in common for the two reactions of this molecule. In this case one expects for it again three observation windows with three time constants. If in the pairs τ_i(COT) and τ_i(BCOD) the difference is smaller than 50%, for example, it will hardly be possible to observe these constants individually (as doubly exponential decays of the apparent L_i), because each window is observed over a limited time only. Instead one will observe an average over τ_i(COT) and τ_i(BCOD).

In fact, this is what was found in the parent ion and mass-78 fragment: The BCOD/COT mixture showed just three time constants, each being probably such an average. Some data with fit curves are shown in the Supporting Information. In addition, there were some oscillations, which seemed identical to those of COT although weaker. The τ_i of the mixture are noticeably shorter than those of COT (Table 1), pointing to a contribution of the minor component. In the table, we give ranges for them, because the values seemed to depend on the data set, in particular on its time span. For example, the value of τ_2(BCOD/COT) was smaller, if the time range investigated (in the parent ion) was shorter. (Such a variation was not feasible with L_1 and L_3.) This may be an indication that the decay of each apparent L_i is actually doubly exponential. Another contribution to the time-range dependence of τ_i may be due to the oscillation, as in COT (Section 3.1). But the variation caused thereby is smaller (5–10 fs, Section 3.1).

In the early attempt to investigate the dynamics of the BCOD/COT mixture [21], the signals (masses 106, 105, 91 and 78) were analyzed independently for each ion and fitted with singly exponential decays with a phenomenological delay time. Three decay times from 48 to 68 fs were reported (and one longer one, see below) [21]. Actually, as each location L_i on the potentials is

Table 1
Simulation parameters for cyclooctatriene and the COT/BCOD mixture: time constants τ_i, oscillation periods T_{osc} with corresponding wavenumber and dephasing times t_d.[a]

	L_1	L_2	L_3
Cyclooctatriene			
Mass 106 (parent ion)	τ_1 = 11 fs, T_{osc1} = 34 fs (980 cm^{-1}), t_{d1} = 18 fs	τ_2 = 67 fs, T_{osc2}, t_{d2} as in mass 78	–
Mass 78	τ_1 = 11 fs, T_{osc1}, t_{d1} as in mass 106	τ_2 = 67 fs, T_{osc2} = 200 fs (167 cm^{-1}), t_{d2} = 70 fs	τ_3 = 190 fs, T_{osc3} = 330 fs (100 cm^{-1}), $t_{d3} \gg \tau_3$
COT/BCOD mixture			
Mass 106	τ_1 = 8–10 fs, T_{osc1}, t_{d1} as in COT	τ_2 = 50–60 fs, T_{osc2}, t_{d2} as in COT	–
Mass 78	τ_1 = 8–10 fs, T_{osc1}, t_{d1} as in COT	τ_2 = 50–60 fs, T_{osc2}, t_{d2} as in COT	τ_3 = 130 fs, T_{osc3}, t_{d3} as in COT

[a] For COT the error limit of τ_1 and τ_2 are estimated to 10%, as the superimposed highly damped oscillations are not trivial to distinguish from decays. The oscillation parameters may be even less precise, as they are typically observed over hardly more than 1 period. In view of the already low signal-to-noise ratio at late times (Fig. 1(b)), the error for τ_3 is estimated to 20%. For the BCOD/COT mixture, we give ranges for τ_1 and τ_2, as the values depend on the duration of the fitted window. The oscillation periods and dephasing times are taken over from COT; the fitted amplitudes were smaller than in COT.

associated with a mass spectrum with more than one peak, identical τ_i should occur in more than one signal, and a decay time τ_i of L_i should occur in the rise ("delay" [21]) of the L_{i+1} signal. With such a consistent analysis, the range 48–68 fs might collapse to that of our τ_2(BCOD/COT) (50–60 fs). The signal from L_1 (with τ_1 and the quickly decaying oscillation) is probably contained in the rise of the parent signal ("delay" 15 fs) of [21]. Our τ_3 was not found in [21], probably because the signal-to-noise ratio of the weak signal tails was not sufficient. On the other hand, an additional time constant (750 fs) is reported for mass 91, which we do not find. However, its existence may be questioned in view of the poor signal-to-noise ratio in the corresponding time range. Whereas we found a pedestal of the fragment signals at long times, no such offset was detected in [21]; this is obviously due to the small probe intensity in [21], which was not sufficient to produce ions from the ground state. Oscillations could not be detected in [21], because the laser pulses were too long (around 100 fs) for this purpose.

Overall, within the limited comparison possibilities, the two investigations seem consistent with each other, with ours revealing more details. Our results on the purified COT also show that the signals from the BCOD/COT mixture with its noticeably shorter time constants are not only due to COT, in contrast to the assumption in [21].

4. Discussion

4.1. Assignments of states and oscillations

The time-dependent signals can be assigned in analogy to the prototype of cyclohexadiene [19] (where the assignment was confirmed by independent methods, see the review [5]) and other molecules, where the wave packet first leaves the FC region (within τ_1), then moves further (during τ_2) on the spectroscopic state ($1B_2$), then (still within τ_2) crosses over to a lower potential ($2A_1$), departing from there within τ_3 to the ground state. This is supported (as in cyclohexadiene [19]) by the fragmentation: From location L_3 (lifetime τ_3) ionization forms no parent anymore; hence this state must already be at considerably lower energy. (The corresponding kinetic energy, that was released, is transferred by vertical ionization to the ion, leading there to fragmentation [19].) By contrast, τ_1 and τ_2 are detected (also) in the parent signal, so that they both must belong to the higher-lying spectroscopic state. Departure from L_3 leads to an even lower state, the ground state ($1A_1$), as to conclude from its long lifetime ($\gg$1 ps, deduced from the constant pedestal of the mass-78 signal) and also from the low probability of dissociative multiphoton ionization by the probe and its stronger dependence on the probe intensity.

Because all lifetimes τ_1–τ_3 are short (comparable to cyclohexadiene), the total process must be barrierless and crossing between the potentials must lead by or through conical intersections (again as in cyclohexadiene [19]).

Our τ_1 and τ_2 of *cyclooctatriene* can be compared with previous values derived by Mathies and coworkers [22]. They determined the fluorescence lifetime from the fluorescence yield and the radiative rate and found τ_{fl} = 30 fs. This is smaller than our residence time on $1B_2$ ($\tau_1 + \tau_2$ = 78 fs). Such a deviation is reasonable, if the optical transition probability decreases on large-amplitude deformation on the path (because the π system is perturbed). In the same work [22] they estimated the $1B_2$ lifetime as the quarter of the period of a ring puckering (ring flattening) vibration (ground-state wavenumber 140 cm^{-1}) that was prominent in the resonance Raman spectrum; the result was 60 fs. (The idea of one quarter of a period is based on the assumption that the exit from $1B_2$ is right at the minimum of this potential.) If the wavenumber of this vibration is by 20% lower in the excited state, the resulting value is in perfect agreement with our $\tau_1 + \tau_2$. Because the resonance in the Raman work involves the $1B_2$ state, one can also conclude that their results support our assignments of the lifetimes τ_1 and τ_2 to the $1B_2$ potential.

The vibrations active in resonance Raman scattering indicate the direction of the initial reaction path, even if the sign of displacements had to be assumed [22]. Similarly, the direction of accelerating slopes can be deduced from coherent oscillations in ground or excited states (see, e.g. [4,35,37,38]). However, as a rule, only few of the Raman active vibrations are observed as coherences [37], and they are typically less accurate in the case of short-lived states. But the Raman-spectroscopic work helps to identify them. Resonant excitation of COT enhanced several low-frequency Raman modes, corresponding to global motions of the ring, as well as CC stretch vibrations [22]. Among the latter, the double-bond stretch (1610 and 1640 cm^{-1}) is beyond our time resolution. However, in L_1 we observed a wavenumber around 950 cm^{-1}, consistent with planar bending of vinylic CH [22], mixed with stretching of the neighboring C–C bonds. (The CH_2–CH_2 stretch, also suggested in [22], cannot be active in the FC region, i.e., in L_1, because the excitation only affects the π electrons.) The 167 cm^{-1} oscillation observed in L_2 is in the range of global ring vibrations [22]. Also in L_3 (on the $2A_1$ surface) there is such an oscillation: its wavenumber (100 cm^{-1}) may correspond to the ground-state value of 140 cm^{-1}, assigned to a ring planarization in [22].

In the *COT/BCOD mixture*, the time constants τ_1 to τ_3 are slightly shorter than for pure COT. Oscillations were also found in all three locations, with the same frequencies but smaller modulation depths in the mixture. As for τ_2, we cannot establish its value from our measurements alone, because the measurement time for the parent did not extend over a full period of the weak oscillation; in this case the fit parameters of exponential decay and oscillation are interdependent. However, the early study of [21] used much longer pulses (100 fs), which average over oscillations; it found a time constant of the same magnitude (48 fs in the parent ion). We can conclude (1) that the minor component (BCOD) does contribute to the signals, (2) that it follows the same type of path over the potentials (spectroscopic state via CI to a dark state, then via a CI to the ground state), and that this path is barrierless and ultrafast.

After the assignment of L_1 (τ_1) to departure from the FC region, L_2 (τ_2) to further relaxation on the spectroscopic state $1B_2$ and L_3 (τ_3) to motion on (and departure from) the dark state $2A_1$, it remains to find out coordinates, i.e. the direction of the relaxation path. Before discussing this path, we first suggest structures for $2A_1/1A_1$ CIs, where the path can branch to products.

4.2. Suggested structures of $2A_1/1A_1$ conical intersections

The formation of benzene + ethylene from BCOD involves a cyclobutane ring cleavage ([2 + 2]-cycloreversion). The same type of reaction but with the other pair of CC bonds being cleaved leads to *Z,Z*-OT. The last CI ($2A_1/1A_1$ CI) for the [2 + 2]-cycloaddition of ethylene to cyclobutane is in common with that for the corresponding cycloreversion. Its structure was calculated by Bernardi and coworkers [39]. It is shown in Scheme 2(a): A pair of CC groups is not only at increased distance but also shifted parallel to each other. (A symmetry-equivalent structure – not shown – involves the other pair of CC groups.) The broken lines can be interpreted as three-electron three-center bonds (formed by one C atom with an opposite pair), a feature frequently met in CIs. It seems plausible that this type of structure applies also to the CI for the two photoreactions of BCOD (Scheme 2(b), with both pairs of CC bonds shown as broken lines, which is short-hand for slightly different structures leading to the two reactions). The two indicated H atoms would in this case be in cis orientation.

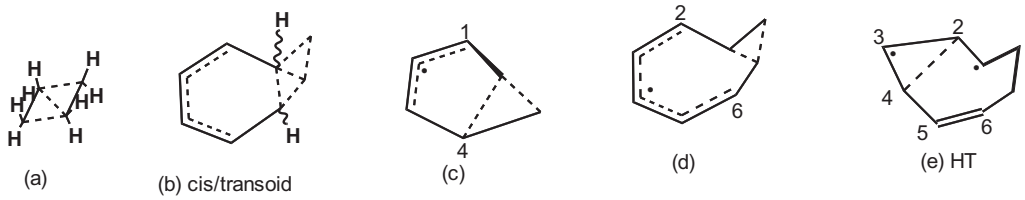

Scheme 2. Structures at $2A_1/1A_1$ conical intersections: (a) CI for cyclobutane ring splitting (ethylene [2 + 2]-cycloaddition) [39], (b) proposed BCOD-like CI with the two hydrogens in cis or transoid orientation, (c) CI for cyclohexa-1,3-diene ring opening [40], (d) proposed CI for ring opening of COT to OT and (e) the Hula-twist (HT) CI with the triangle 2-3-4 folded from the plane 1-2-4-5-6 of the remaining π system [8].

But this structure has also an interesting relationship with the CI for cyclo*hexa*diene ring opening, as calculated also by the Bernardi group [40]. In this case, one CH_2 (C6) group has not only increased its distance from the other CH_2 (C5) group but is also slightly shifted towards C4 as in a beginning ring contraction (Scheme 2(c)). (These two coordinates also span the branching space.) Again there is a three-electron three-center bond, with a fourth electron delocalized over the ring [40]. We suggest a similar structure for the CI responsible for cyclo*octa*triene ring opening: one CH_2 (C7) group with increased distance from the other and shifted parallel to the opposite CH–CH_2 (C8–C1) bond (Scheme 2 (d)). This looks very similar to what is sketched in Scheme 2(b): The difference is that in CI_b there is an additional (weak) bond between C1 and C6. To form such a bonding interaction in excited COT, the two ends of the COT π system (C1 and C6) must rotate in conrotatory direction, so that the two hydrogens move towards trans orientation. Because in a fully developed trans configuration the fused cyclobutane would increase the strain, the two CH bonds will form an angle <180°; therefore this CI is called "transoid" in Scheme 2(b). Due to the increasing strain, the decay from this CI is expected to disfavor (trans-) BCOD but instead leads to benzene + ethylene besides recovery of COT.

Hence for the pericyclic reactions of COT (ring opening and cleavage), we suggest two different CIs (CI_d and $CI_{b,transoid}$). Their geometrical structures seem rather close together. Therefore the paths to them probably branch only late and the energetics may be also similar, so that these channels may be hardly distinguishable in the experiment. This is expected to be different for a path via a third CI (CI_{HT}, Scheme 2(e), corresponding to the structure calculated in [8] for open-chain polyenes), leading to Z,E-isomerization. Such a rearrangement must in a ring be of Hula-twist type, in which a C=C and a neighboring C–C bond are both twisted (or C3 rotates around an axis connecting C2 and C4); in the CI_{HT} this rotation is <90° [8]. On this path the central double bond is strongly twisted, whereas in the two pericyclic reactions it is not affected. The strong geometrical difference between CI_{HT} and the pericyclic CIs on the other side suggests that the paths to them originate from an early branching.

It may be worth mentioning that one of the suggested CIs also rationalizes two side products, which are considered the only other primary products from COT [15]: From a structure very close to CI_{HT} (Scheme 2(e)), recoupling [40] the electron at C1 with that at C4 and correspondingly C2 with C3 leads to bicyclo[4.2.0]octa-2,5-diene (i.e., electrocyclic ring closure of the diene part of COT to a cyclobutene derivative), whereas 1–3 and 2–6 recoupling leads to tricyclo[3.3.0.02,8]oct-2-ene.

Scheme 3 summarizes the paths from excited COT to the suggested CIs. It indicates an early branching between Z,E-isomerization and pericyclic rearrangement and a late branching to the two pericyclic CIs (CI_d and $CI_{b,transoid}$). As the reaction COT → benzene + ethylene (via $CI_{b,transoid}$) requires a complicated rearrangement of five electron pairs, it seems plausible that not all of them occur synchronously. Instead, the system perhaps moves first in the direction to CI_d, during which also the CH_2–CH_2 bond becomes

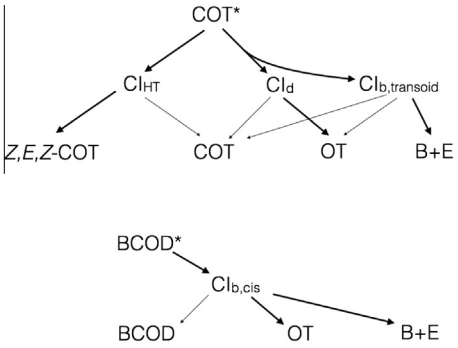

Scheme 3. Proposed paths of excited COT and BCOD via different $2A_1/1A_1$ CIs to the various products. "B+E" stands for benzene + ethylene. From excited COT, we suggest an early branching to Hula twist (HT) and the pericyclic path and only late on the latter a branching to CI_d and $CI_{b,transoid}$, whereas from BCOD* there is only a late branching.

weaker; this may facilitate conrotatory approach of C1 and C6 in an asynchronous but concerted process. This is indicated in Scheme 3 by the bent arrow.

The corresponding interconnections for BCOD are also shown in Scheme 3. In this case, no branching is required on the excited state surfaces. The close relationship between $CI_{b,cis}$ and $CI_{b,transoid}$ rationalizes why COT and BCOD have some photoproducts (those of pericyclic reactions) in common. But the two CI_b cannot be identical and must even be separated by a barrier: If there were a common CI_b reached from both COT* and BCOD*, then one should find BCOD as a photoproduct of COT and similarly COT as a product of BCOD, in contrast to the results of matrix spectroscopy [12].

4.3. The paths on the potentials and the time-resolved signals

As already said (Section 4.1), the signals point to the usual scheme in photochemical pericyclic reactions and cis–trans isomerization: Within τ_1 the molecule escapes from the FC region, within τ_2 it moves further on the spectroscopic surface $1B_2$ and leaves from it, going around a CI to the dark surface $2A_1$, where during τ_3 it continues its path and leaves it through the last CI. However, we expected several photoreactions with the branchings described above (Section 4.2). So, should one not expect more time constants? The answer also depends on whether the branching occurs early or late.

To distinguish the two cases, it should be noted that a branching from a reactant R to two products P_1 and P_2, produced with rate constants k_1 and k_2, gives rise to only one observable time constant $\tau = (k_1 + k_2)^{-1}$; both products appear within the same time as the reactant disappears. However, if the branched process is followed by consecutive reactions from P_1 and P_2, these (parallel) reactions give rise to two independent additional time constants. Hence in the case of COT the suggested early branching (e.g. near the FC region) to Z–E isomerization and pericyclic reactions may be

recognized from later steps (e.g. the departure from the 2A surface; P_1 and P_2 can then represent separate minimum-energy CIs). By contrast, the late branching of COT to two pericyclic reactions will not be observable in the excited states; in the ground state (after leaving L_3) there was no observed time dependence. Also the late branching in BCOD will not give rise to additional time constants.

But in spite of the expectation, COT shows the signature (i.e., the three time constants) of only one reaction channel. There can be several reasons, why additional time constants (in L_3, or also in L_2) elude observation:

(1) It is just too difficult to extract an additional time constant τ_3' besides τ_3, in particular in the presence of the oscillation and in the view of the limited time window. This is also demonstrated by the BCOD/COT mixture, where in spite of the presence of two substances there was only one time constant (certainly an average over the two components) in every location.
(2) The expected two time constants may be too similar, so that they cannot be separated in the limited time windows. An average of them would then result from the fit. Again the BCOD/COT mixture can serve as an example.
(3) The ionization probability from one of the paths may be much lower than from the other.

If (1) or (2) is the main reason, we must postulate that also the oscillation in L_3 is accidentally the same in the two channels (which seems not very probable) or is lacking in one of them. This is a hint that the third interpretation should be preferred. In fact, in cyclo-octadiene and -heptadiene [20] the ionization probability from the cis–trans channel is 10 times smaller than from the electrocyclic ring closure to cyclobutene derivatives. This factor would already overcompensate the probability ratio (4:1) of Z–E isomerization over pericyclic reactions, and it might be even larger in the COT case. The reason may be that double-bond torsion interrupts the conjugated π system, so that the ionization energy will rise and the multiphoton ionization probability will drop. By contrast, ring opening to OT extends the π system. (In fact, the ionization energy of *E*,*E*-OT is lower – 7.8 eV [41] – than that of COT (8.4 eV [33]). That of *Z*,*Z*-OT seems unknown, but is certainly similar.)

A further hint is the ground-state signal, i.e. the pedestal after leaving L_3. If it were the product *mono-E*-COT, it should isomerize in the ground state within very few picoseconds, accelerated from the room-temperature lifetime of milliseconds [12] by the released excess energy, similarly as in *mono-E*-cycloheptadiene [20]. The constant signal thus points to the longer-lived *Z*,*Z*-OT (seconds at room temperature [12]), the product of electrocyclic ring opening.

Another support comes from BCOD, which only undergoes pericyclic reactions. Although it was present with only 20% in the BCOD/COT mixture, the signals from it were strong enough to compete with those of COT. This becomes clear, if only 20% of the COT wave packets (namely those in the pericyclic channel) are detected, whereas the 80% on the Z–E path are invisible.

It hence seems probable that in the time-resolved data of COT we only see the pericyclic channels, not the Z–E isomerization.

4.4. Interpretation in terms of driving forces

The analysis of resonance Raman intensities in [22] revealed a combination of several coordinates as the direction of the initial motion. Most important are C=C stretching, several low-wavenumber delocalized modes leading to ring flattening (symmetry a_1, for example, 140 cm^{-1}) and others (symmetry a_2, e.g., 404 cm^{-1}) that involve twisting of the central double bond. From the observed Raman intensities, the displacement of the $1B_2$ minimum was calculated [22], resulting in a C=C torsion angle of ca. 50°. (This strong torsion of the central double bond was the reason that we assigned in Scheme 1 the product *mono-E*-COT [12] to *Z*,*E*, *Z*-COT.) Lawless et al. interpreted the ring flattening as an indication that pericyclic reactions (they only considered electrocyclic ring opening of COT) require a certain planarity of the ring [22]. They also suggested that motion towards Woodward-Hoffman active coordinates only begins in the dark state. As another example they mention cycloheptatriene, where ring flattening precedes sigmatropic H migration.

However, in this picture the C=C torsion in COT is confusing: With its a_2 symmetry, it is a conrotatory deformation (in planar geometry), whereas the COT → OT ring opening is generally believed to be disrotatory. Our description seems to us more satisfactory in this respect:

The molecule will first move along FC active coordinates. As the excitation of the conjugated π system changes the double-bond character, bond lengths in this system will change, the torsion of the single bonds will be reduced (leading to a distortion of the ring towards planarization of the π system) and double bonds can also twist. These deformations are not necessarily simultaneous but can also be alternative. Thus we suggest that molecules leaving the FC region with C=C twist continue their motion towards Z–E isomerization, whereas those without this twist but with the other deformations will follow the pericyclic channel. This is consistent with the early branching shown in Scheme 3. In this interpretation Lawless et al. [22] have observed the Raman signals from two different reaction channels.

Decrease of the single-bond torsional angles will not only tend to planarize the ring (actually the π system) but also increase the ring strain and thus in particular weaken the CH_2–CH_2 bond (which is out of plane). This raises the σ orbital and lowers the σ^* orbital, so that they better interact with the π system. (The geometrical orientation is already suitable, see Fig. 7 of [22].) In this way the pericyclic interactions are now activated, and the molecule will turn to such a direction. In contrast to [22], we suggest that this already happens on the spectroscopic surface (consistent with the appearance of a second observation window on $1B_2$ in our signals): Only on sufficient deformation in the WH direction the two-electron excited $2A_1$ surface is lowered sufficiently that it can cross with the $1B_2$ potential at low energy.

It is worth noting that limiting the excursion in WH direction e.g. by a stiff backbone will again lift the $1B_2$ surface already at small deformation and therefore will result in an intersection (CI) with $2A_1$ at higher energy. In this case, departure from $1B_2$ will require activation energy, and the $1B_2$ lifetime will be longer. This explains for the first time, why stiff cyclohexadiene derivatives such as 7-dehydrocholesterol have remarkably long $1B_2$ lifetimes (near 1 ps, review in [6]), so that they can even fluoresce. Similar effects can be expected, if the excitation is too much "diluted" (delocalized), so that down-slopes are only small and excursions remain limited.

Driving forces can also rationalize another observation, namely that the Z–E isomerization is surprisingly efficient, although it gives rise to a very strained product. Driving forces are down-slopes of the potentials. It was argued in [9], if a molecule is predistorted in the ground state in a direction, which has a component of a photochemically active coordinate (such as C=C torsion), vertical excitation places the molecule to a down-slope on the upper potential, which accelerates the wave packet selectively into this direction (on expense of an alternative photochemical path). In the case of Hula-twist isomerization (that must apply to cyclic systems), which twists two neighboring bonds, a pretwist of the single bond (see the COT formula in Scheme 1) is already sufficient to enhance this channel [9]. The widespread efficiency of Z–E isomerization of cyclic dienes was rationalized in this way [9].

4.5. Concerted or not?

The question, whether a reaction is concerted or stepwise, is usually decided by checking the stereochemistry of substituted derivatives. In a stepwise process, there is an intermediate diradical (singlet or triplet) of sufficient lifetime (several hundred femtoseconds or more), so that one group can perform an internal rotation. In COT ring opening to OT, an intermediate diradical is hardly conceivable; it would lead to a mixture of Z and E isomers. In the experiment, the only primary open-chain isomer observed was *Z,Z*-OT [12]. Hence it seems clear that this reaction must be concerted. (For the COT Z–E isomerization, there is no such question, since there is only one electron pair, which is decoupled and recoupled.)

The question is, however, not so easy to answer for the cleavage of the four-membered ring of BCOD. Kaupp et al. presented stereochemical evidence for a stepwise cleavage of BCOD derivatives [42] and other annelated cyclobutanes [43,44] (see also the brief survey on p. 145–6 of [45]). They even formulated the rule ("cis effect") that the maximum release of steric strain controls, which of the four cyclobutane bonds opens first [43]. The intermediate diradicals were singlets [46]. The [2 + 2]-cycloreversion review [47] quotes a few more examples, where stereochemical retention was not perfect. On the other hand, there are cleavages of cyclobutane rings at cryogenic temperatures such as in the preparation of cyclobutadiene (from a propellane-type derivative of BCOD at 7 K [48]); so, the reaction must be barrierless and hence ultrafast till the end. This leaves no time for internal rotation of any intermediate, if there were any.

For interpretation of the difference, it may be important to notice that the derivatives investigated by Kaupp [42–44] had substituents, which can stabilize a radical center of an intermediate. This can give rise to a minimum on the potential (probably in the ground and excited state), before opening of the second bond, and thus to an intermediate. The cleavage of the second bond would occur on the ground-state surface.

In principle one could distinguish concerted and stepwise reactions by ultrafast spectroscopy: A stepwise process would pass through the last conical intersection and then exhibit a step with sufficient lifetime (e.g. >500 fs) on the ground-state surface to allow for internal rotation. It would thus be desirable to investigate the pure BCOD at correspondingly long delay times and good signal-to-noise ratio.

However, Scheme 3 suggests that all products of BCOD originate from the same CI (or very similar ones, see also Scheme 2). One of them, *Z,Z*-OT, is most probably produced in a concerted way, because a radical intermediate would also give rise to E isomers of OT. Therefore it seems reasonable that this is also the case for the other products (benzene + ethylene).

It is also worth noting that the reverse reaction, [2 + 2]-cycloaddition, was found to be ultrafast (hence concerted) in cases, where the two ethylenic parts are suitably preoriented (norbornadiene [49], pyrimidine dimerization in di- and polynucleotides [50,51], in a substituted cyclophane [52]).

5. Conclusion

As summarized in the following, in particular cyclooctatriene confirms several general rules on the excited potentials involved and their conical intersections, the directions of the paths (with suggested branchings) and the driving forces. It also in part supplements the rationalization of these rules. In BCOD the ultrafast data and other evidence supports the idea that the ring of the unsubstituted compound splitting is concerted, although in some derivatives it is stepwise.

(1) The time-resolved data for COT fit into the general scheme for both, pericyclic photoreactions and cis–trans photoisomerization: the wave packet moves over two excited-state surfaces and via two consecutive CIs. In the first observation window (L_1, $\tau_1 = 11$ fs), it leaves the FC region, then (L_2, $\tau_2 = 67$ fs) it continues its path on the spectroscopic surface ($1B_2$) and leaves it around a CI to the dark surface ($2A_1$), where (L_3) it further moves and then departs through a CI to the ground-state surface ($1A_1$) within $\tau_3 = 190$ fs. On $1A_1$, no further time dependence is found over 6 ps, from which we conclude that the observed product is not the strained *mono-E*-COT, which would rearrange in this time scale. All time constants are short enough to conclude that the path on the excited-state surfaces is barrierless.

(2) Also the idea of driving forces works in the rather complicated case of COT: Initial excitation accelerates the wave packet along FC active coordinates. This not only changes bond lengths in the conjugated π system but also torsion angles. This triggers two *alternative* (not recognized in [22]) channels (i.e. a branching in the FC region); signatures of both were – in our interpretation – observed in resonance Raman spectroscopy [22]. One of them, with its strong increase of double-bond torsion, ultimately leads to Hula-twist Z–E isomerization; its efficiency [12] is enhanced by the pretwist of the neighboring single bond [12]. The other reduces the C–C torsion, thereby planarizes the π system and increases the strain of the CH_2–CH_2 bond (which has already a suitable orientation), which in turn activates the Woodward–Hoffmann-type σ–π interactions. We suggest two geometrically similar CIs (hence a late branching) for the two observed pericyclic reactions, ring opening to OT and cleavage to benzene + ethylene [12].

(3) That is, the WH rules are not yet known to the molecule immediately after excitation but are activated only by deformation along FC-active coordinates, as we pointed out previously. This deformation sometimes just provides the geometric conditions to facilitate the necessary σ–π interactions; now we draw the attention also to the increased σ strain, which energetically approaches the σ and σ^* orbitals to appropriate π and π^* orbitals. The WH-type deformation is thus initiated already on the spectroscopic surface (in L_2). Only if this is the case and the excursion in this direction is large enough, the two-electron excited dark state is lowered sufficiently to intersect the one-electron excited bright state at low energy. If the excursion is limited by a stiff backbone (or if the excited π system is too much delocalized), the CI is at higher energy, so it can be reached only with activation energy (Section 4.4). This explains, why molecules like 7-dehydrocholesterol (a steroid cyclohexadiene derivative) has a longer $1B_2$ lifetime and can even fluoresce (review in [6]).

(4) The (Hula-twist) Z–E isomerization is the dominant photoreaction, 80% of the products being the strained *mono-E*-COT [12]. As said above, we consider this surprising efficiency to be caused by the pretwist of the neighboring single bond, which is enhanced in the excited state; the amplification of predistortion was recently suggested to rationalize many phenomena in photochemistry [9].

As COT undergoes the three main photoreactions just mentioned, more than one set of three time constants was expected. The two pericyclic channels are suggested to branch only just before the last CI, on transition to the ground-state surface; therefore they have a common path on the excited potentials. However, this pericyclic path and the path towards Z–E isomerization separate already in the FC region, as suggested, (1) because a common

CI is geometrically hardly conceivable and (2) because the idea is supported by resonance Raman spectroscopy, which yielded the (two alternative) coordinates of initial motion [22].

Several reasons are conceivable, why we detected only one path: (1) In view of the oscillations detected in L_1–L_3 with several fit parameters each, it is just hard to detect more components, in fact, there were no oscillations in previous cases, where we detected an early branching (such as in cyclooctadiene [20]). (2) The time constants for the two paths might be rather similar; in fact, the BCOD/COT mixture presents an example: the measured time constants are probably a weighted average of those of the two components. (3) The ionization probability from the Z–E path is substantially lower than from the other. Whereas we prefer the latter rationalization for several reasons (see Section 4.3), it is also possible that all three contribute.

Also the data for BCOD seem consistent (as far as is possible to judge from the BCOD/COT mixture) with the scheme with two excited states and two conical intersections. As we suggest a late branching to the products, only one set of time constants was expected. As in COT, the process is barrierless (to conclude from the short time constants). This suggests a concerted reaction also for the ring cleavage to benzene + ethylene, whereas a stepwise reaction was observed in some substituted derivatives [42,43]. On the other hand, a slower second step (on the ground-state surface) could have eluded the measurements; a better experimental check would use pure BCOD.

The last CI suggested for this ring cleavage is identical – or nearly so – with that for the (concerted, see Section 4.5) ring opening to OT. This again suggests that also the ring cleavage is not stepwise in unsubstituted BCOD. Furthermore, in some BCOD derivatives, the ring cleavage works at liquid-helium temperatures (Section 4.5), implying that the complete process is barrierless and hence concerted. Quantum chemical calculations would certainly be desirable to check this question and the proposed structures of the various CIs of BCOD and COT as well as the suggested barrier between $CI_{b,cis}$ and $CI_{b,transoid}$. They could also further clarify, why the reactions investigated here are barrierless, whereas isomerization of *E*,*E*-octatetraene has a minor barrier before the last CI [53–55].

Conflict of interest

There is no conflict of interest.

Acknowledgement

This work was supported by the Deutsche Forschungsgemeinschaft (Project FU 363/1).

Appendix A. Supplementary data

Supplementary data associated with this article can be found, in the online version, at http://dx.doi.org/10.1016/j.chemphys.2015.10.007.

References

[1] M. Klessinger, J. Michl, Excited States and Photochemistry of Organic Molecules, VCH, New York, 1995.
[2] M. Garavelli, C.S. Page, P. Celani, M. Olivucci, W.E. Schmid, S.A. Trushin, W. Fuß, J. Phys. Chem. A 105 (2001) 4458.
[3] P. Celani, S. Ottani, M. Olivucci, F. Bernardi, M.A. Robb, J. Am. Chem. Soc. 116 (1994) 10141.
[4] K. Kosma, S.A. Trushin, W. Fuß, W.E. Schmid, Phys. Chem. Chem. Phys. 11 (2009) 172.
[5] S. Deb, P.M. Weber, Annu. Rev. Phys. Chem. 62 (2011) 19.
[6] B.C. Arruda, R.J. Sension, Phys. Chem. Chem. Phys. 16 (2014) 4439.
[7] W. Fuß, S. Lochbrunner, A.M. Müller, T. Schikarski, W.E. Schmid, S.A. Trushin, Chem. Phys. 232 (1998) 161.
[8] D. Sampedro Ruiz, A. Cembran, M. Garavelli, M. Olivucci, W. Fuß, Photochem. Photobiol. 76 (2002) 622.
[9] W. Fuß, J. Photochem. Photobiol. A 297 (2015) 45.
[10] K. Kosma, S.A. Trushin, W. Fuß, W.E. Schmid, J. Phys. Chem. A 112 (2008) 7514.
[11] T.D. Goldfarb, L. Lindqvist, J. Am. Chem. Soc. 89 (1967) 4588.
[12] P. Datta, T.D. Goldfarb, R.S. Boikess, J. Am. Chem. Soc. 91 (1969) 5429.
[13] B.E. Kohler, Chem. Rev. 93 (1993) 41.
[14] W.R. Roth, B. Peltzer, Liebigs Ann. Chem. 685 (1965) 56.
[15] B.H.O. Cook, W.J. Leigh, in: Z. Rappoport (Ed.), The Chemistry of Dienes and Polyenes, Wiley, New York, 2000, pp. 197–255.
[16] A.C. Cope, A.C. Haven Jr., F.L. Ramp, E.R. Trumbull, J. Am. Chem. Soc. 74 (1952) 4867.
[17] J.M. Greathead, S.W. Orchard, Int. J. Chem. Kinet. 15 (1983) 1069–1080.
[18] A.C. Cope, F.A. Hochstein, J. Am. Chem. Soc. 72 (1950) 2515.
[19] W. Fuß, W.E. Schmid, S.A. Trushin, J. Chem. Phys. 112 (2000) 8347.
[20] W. Fuß, S. Panja, W.E. Schmid, S.A. Trushin, Mol. Phys. 104 (2006) 1133.
[21] A.M. Müller, Ultrafast reaction dynamics of polyatomic molecules probed by ionization, Max-Planck-Institut für Quantenoptik, Univ. München, Garching, 2001, ftp://ftp.ipp-garching.mpg.de/pub/mpq/MPQ257.pdf, <http://edoc.ub.uni-muenchen.de/524/>.
[22] M.K. Lawless, R.A. Mathies, J. Chem. Phys. 100 (1994) 2492.
[23] M.K. Lawless, S.D. Wickham, R.A. Mathies, J. Am. Chem. Soc. 116 (1994) 1593.
[24] M.K. Lawless, S.D. Wickham, R.A. Mathies, Acc. Chem. Res. 28 (1995) 493.
[25] P.J. Reid, M.K. Lawless, S.D. Wickham, R.A. Mathies, J. Phys. Chem. 98 (1994) 5597.
[26] P.J. Reid, S.J. Doig, R.A. Mathies, J. Phys. Chem. 94 (1990) 8396.
[27] B.M. Goodson, C.-Y. Ruan, V.A. Lobastov, R. Srinivasan, A.H. Zewail, Chem. Phys. Lett. 374 (2003) 417.
[28] F.A.L. Anet, I. Yavari, Tetrahedron Lett. 6 (1975) 4221.
[29] F.A.L. Anet, I. Yavari, Tetrahedron 34 (1978) 2879.
[30] S.A. Trushin, W. Fuß, K. Kosma, W.E. Schmid, Appl. Phys. B 85 (2006) 1.
[31] N.F. Scherer, L.R. Khundkar, T.S. Rose, A.H. Zewail, J. Phys. Chem. 91 (1987) 6478.
[32] S.A. Trushin, W. Fuß, W.E. Schmid, K.L. Kompa, J. Phys. Chem. A 102 (1998) 4129.
[33] C. Batich, P. Bischof, E. Heilbronner, J. Electron. Spectrosc. Relat. Phenom. 1 (1973) 333.
[34] T. Yatsuhashi, S.A. Trushin, W. Fuß, W. Rettig, W.E. Schmid, S. Zilberg, Chem. Phys. 296 (2004) 1.
[35] S.A. Trushin, K. Kosma, W. Fuß, W.E. Schmid, Chem. Phys. 347 (2008) 309.
[36] W. Fuß, W.E. Schmid, S.A. Trushin, Chem. Phys. Lett. 342 (2001) 91.
[37] W. Fuß, W.E. Schmid, K.K. Pushpa, S.A. Trushin, T. Yatsuhashi, Phys. Chem. Chem. Phys. 9 (2007) 1151.
[38] S.A. Trushin, W. Fuß, W.E. Schmid, Chem. Phys. 259 (2000) 313.
[39] F. Bernardi, S. De, M. Olivucci, M.A. Robb, J. Am. Chem. Soc. 112 (1990) 1737.
[40] F. Bernardi, M. Olivucci, M.A. Robb, Chem. Soc. Rev. 25 (1996) 321.
[41] T.B. Jones, J.P. Maier, Int. J. Mass Spectrom. Ion Phys. 31 (1979). 287-201.
[42] G. Kaupp, E. Jostkleigrewe, Angew. Chem. 88 (1976) 812.
[43] G. Kaupp, M. Stark, H. Fritz, Chem. Ber. 111 (1978) 3624.
[44] G. Kaupp, W.H. Laarhoven, Tetrahedron Lett. 12 (1976) 941.
[45] W.H. Laarhoven, in: A. Padwa (Ed.), Organic Photochemistry, Marcel Dekker, New York, 1987, pp. 129–224.
[46] G. Kaupp, Angew. Chem. 85 (1973) 766.
[47] E. Schaumann, R. Ketcham, Angew. Chem. Int. Ed. 21 (1982) 225.
[48] S. Masamume, F.A. Souto-Bachiller, T. Machiguchi, J.E. Bertie, J. Am. Chem. Soc. 100 (1978) 4889.
[49] W. Fuß, K.K. Pushpa, W.E. Schmid, S.A. Trushin, Photochem. Photobiol. Sci. 1 (2002) 60.
[50] W.J. Schreier, J. Kubon, P. Clivio, W. Zinth, P. Gilch, Spectroscopy 24 (2010) 309.
[51] W.J. Schreier, J. Kubon, N. Regner, K. Haiser, T.E. Schrader, W. Zinth, P. Clivio, P. Gilch, J. Am. Chem. Soc. 139 (2009) 5038.
[52] R.Y. Brogaard, A.E. Boguslavskiy, O. Schalk, G.D. Enright, H. Hopf, V.A. Raev, P.G. Jones, D.L. Thomsen, T.I. Sølling, A. Stolow, Chem. Eur. J. 17 (2011) 3922.
[53] Y.S. Choi, T.-S. Kim, H. Petek, K. Yoshihara, R.L. Christensen, J. Chem. Phys. 100 (1994) 9269.
[54] H. Petek, A.J. Bell, Y.S. Choi, K. Yoshihara, B.A. Tounge, R.L. Christensen, J. Chem. Phys. 102 (1995) 4726.
[55] M. Garavelli, P. Celani, N. Yamamoto, F. Bernardi, M.A. Robb, M. Olivucci, J. Am. Chem. Soc. 118 (1996) 11656.